00029404 Cell

An Innexin-Dependent Cell Network Establishes Left-Right Neuronal Asymmetry in *C. elegans*

Chiou-Fen Chuang,[1,3] Miri K. VanHoven,[1] Richard D. Fetter,[1] Vytas K. Verselis,[2] and Cornelia I. Bargmann[1,*]
[1] Howard Hughes Medical Institute, The Rockefeller University, 1230 York Avenue, New York, NY 10021, USA
[2] Department of Neuroscience, Albert Einstein College of Medicine, Bronx, NY 10461, USA
[3] Present address: Division of Developmental Biology, Cincinnati Children's Hospital Research Foundation, Cincinnati, OH 45229, USA.
*Correspondence: cori@rockefeller.edu
DOI 10.1016/j.cell.2007.02.052

SUMMARY

Gap junctions are widespread in immature neuronal circuits, but their functional significance is poorly understood. We show here that a transient network formed by the innexin gap-junction protein NSY-5 coordinates left-right asymmetry in the developing nervous system of *Caenorhabditis elegans*. *nsy-5* is required for the left and right AWC olfactory neurons to establish stochastic, asymmetric patterns of gene expression during embryogenesis. *nsy-5*-dependent gap junctions in the embryo transiently connect the AWC cell bodies with those of numerous other neurons. Both AWCs and several other classes of *nsy-5*-expressing neurons participate in signaling that coordinates left-right AWC asymmetry. The right AWC can respond to *nsy-5* directly, but the left AWC requires *nsy-5* function in multiple cells of the network. NSY-5 forms hemichannels and intercellular gap-junction channels in *Xenopus* oocytes, consistent with a combination of cell-intrinsic and network functions. These results provide insight into gap-junction activity in developing circuits.

INTRODUCTION

Developing neurons and other embryonic cell types are often connected by gap junctions, intercellular channels that allow the direct transfer of electrical signals and small molecules between coupled cells (Bennett and Zukin, 2004). A gap junction is formed by aligned homotypic or heterotypic half-junctions on two adjacent cells and can be composed of either connexins, which are present only in chordates, or innexins or pannexins, which are present in all metazoa. Developing neurons in the vertebrate spinal cord, retina, and cortex are interconnected by gap junctions that fade away later in life (Kandler and Katz, 1995). The connected neurons form functional domains with coordinated patterns of spontaneous activity and intracellular calcium flux (Yuste et al., 1995). Transient gap-junction networks have been proposed to regulate proliferation, migration, cell death, contact inhibition, and synapse formation and/or elimination, but there is little direct evidence of their function. Their best understood role is in developing motor neurons, where they potentiate the synaptic refinement that leads to the selection of a single input neuron per muscle fiber (Chang et al., 1999). In addition, mutations in gap-junction genes eliminate certain chemical synapses in the *Drosophila* optic lamina, suggesting that signals for synapse formation may pass through gap junctions (Curtin et al., 2002).

Gap junctions link the earliest born nonneuronal cells in embryos and are essential for *C. elegans*, *Drosophila*, and mammalian embryogenesis (Phelan, 2005; Wei et al., 2004). The first detectable left-right asymmetry of the body axis in frog and chick embryos is generated by gap junctions (Levin and Mercola, 1999). This asymmetry predicts the laterality of the Shh and BMP signaling pathways that generate asymmetry in internal organs.

Both invariant and random left-right asymmetries are present in the nervous system of the nematode *Caenorhabditis elegans* (Hobert et al., 2002). Most left-right asymmetries are tightly coupled to the body axis, but left-right differences between the AWC olfactory neurons, which are distinguished as AWC^{ON} or AWC^{OFF} based on whether or not they express the reporter *str-2::GFP*, are stochastic. Each animal generates one AWC^{ON} neuron and one AWC^{OFF} neuron, but half of the animals express *str-2* in the right AWC neuron while the other half express *str-2* in the left AWC (Troemel et al., 1999). Cell-killing experiments suggest that AWC^{OFF} is the default state and that induction of AWC^{ON} requires an interaction between the AWC neurons. Genetic studies of symmetric mutants with two AWC^{ON} or two AWC^{OFF} neurons have defined a calcium-dependent kinase cascade that regulates AWC asymmetry near the time of synapse formation, including

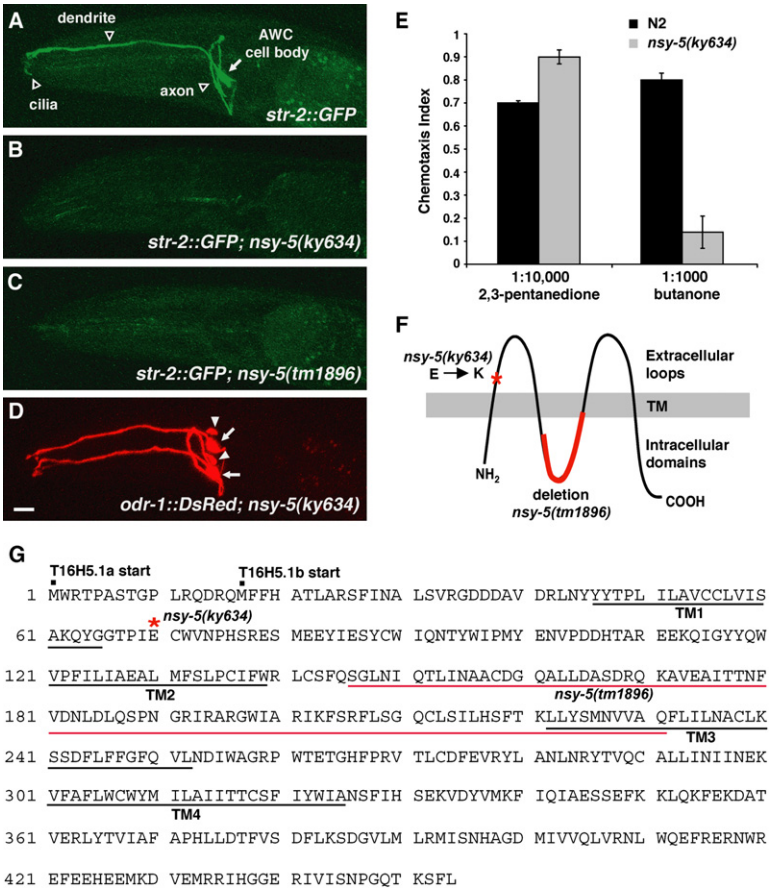

Figure 1. *nsy-5* Encodes an Innexin Gap-Junction Protein

(A–C) Expression of *str-2::GFP* in wild-type and *nsy-5* mutant animals.

(D) Expression of *odr-1::DsRed* in a *nsy-5(ky634)* mutant. Arrows indicate the AWC cell body; arrowheads indicate the smaller AWB cell body. All images are confocal projections. Anterior is at left; ventral is down. Scale bar = 10 μm.

(E) Chemotaxis assays. A chemotaxis index of 1 represents 100% of animals approaching the odor; a chemotaxis index of 0 represents random behavior. Error bars indicate standard error of the mean.

(F) Predicted structure of NSY-5 protein encoded by T16H5.1a.

(G) Amino acid sequence of NSY-5, indicating location of transmembrane domains (TM1–4), the G→A (E70K) change in the *nsy-5(ky634)* allele, and the in-frame deletion in the *nsy-5(tm1896)* allele.

a voltage-activated calcium channel, the calcium-dependent kinase CaMKII, and a MAP kinase cassette (Chuang and Bargmann, 2005; Sagasti et al., 2001; Tanaka-Hino et al., 2002; Troemel et al., 1999). The earliest signaling molecule in this cascade is NSY-4, a transmembrane protein related to vertebrate claudin adhesion proteins and regulatory γ subunits of voltage-activated calcium channels (VanHoven et al., 2006). Axon guidance mutants disrupt AWC asymmetry, but classical synaptic communication is not essential, suggesting that a different kind of cell communication is involved (Troemel et al., 1999).

Here we analyze the signaling between AWC neurons by characterizing an AWC asymmetry gene, *nsy-5*, that encodes a member of the innexin/pannexin family of gap-junction proteins. We show that AWC neurons belong to a transient neuronal network connected by *nsy-5*-dependent junctions and that this network coordinates communication between AWC^{OFF}, AWC^{ON}, and other neurons to generate left-right asymmetry.

RESULTS

nsy-5 Encodes an Innexin Homolog Required for AWC Asymmetry

nsy-5(ky634) was identified in a genetic screen for mutants that do not express *str-2::GFP* in either AWC cell (Figures 1A and 1B; Figure 2A). This 2 AWC^{OFF} phenotype can be caused by mutations that affect general AWC fate, axon guidance, signaling between AWC neurons, or activity-dependent maintenance of the *str-2::GFP* reporter (Troemel et al., 1999). AWC fate appeared to be normal in *nsy-5(ky634)* mutants based on the bilateral expression of the AWC marker *odr-1::DsRed*, and the same marker revealed apparently normal AWC axons, dendrites, and cilia (Figure 1D). The *str-2::GFP* expression defect was observed at all developmental stages, unlike the late-onset defect in the maintenance mutants (Troemel et al., 1999). These results suggest that *nsy-5* affects the establishment of left-right asymmetry of AWC neurons.

nsy-5 animals did not chemotax to the odorant 2-butanone, which is sensed by AWC^{ON}, but responded normally to the odorant 2,3-pentanedione, which is sensed by AWC^{OFF} (Wes and Bargmann, 2001) (Figure 1E). These results support the idea that *nsy-5* mutants have one or more functional AWC^{OFF} neurons but no functional AWC^{ON} neurons.

nsy-5(ky634) was mapped to a small interval on the first chromosome, and the mutant phenotype was rescued with an 18 kb PCR product of genomic DNA containing only one full-length open reading frame, T16H5.1/*inx-19* (Figure 3, row 1). T16H5.1 encodes two innexin-related

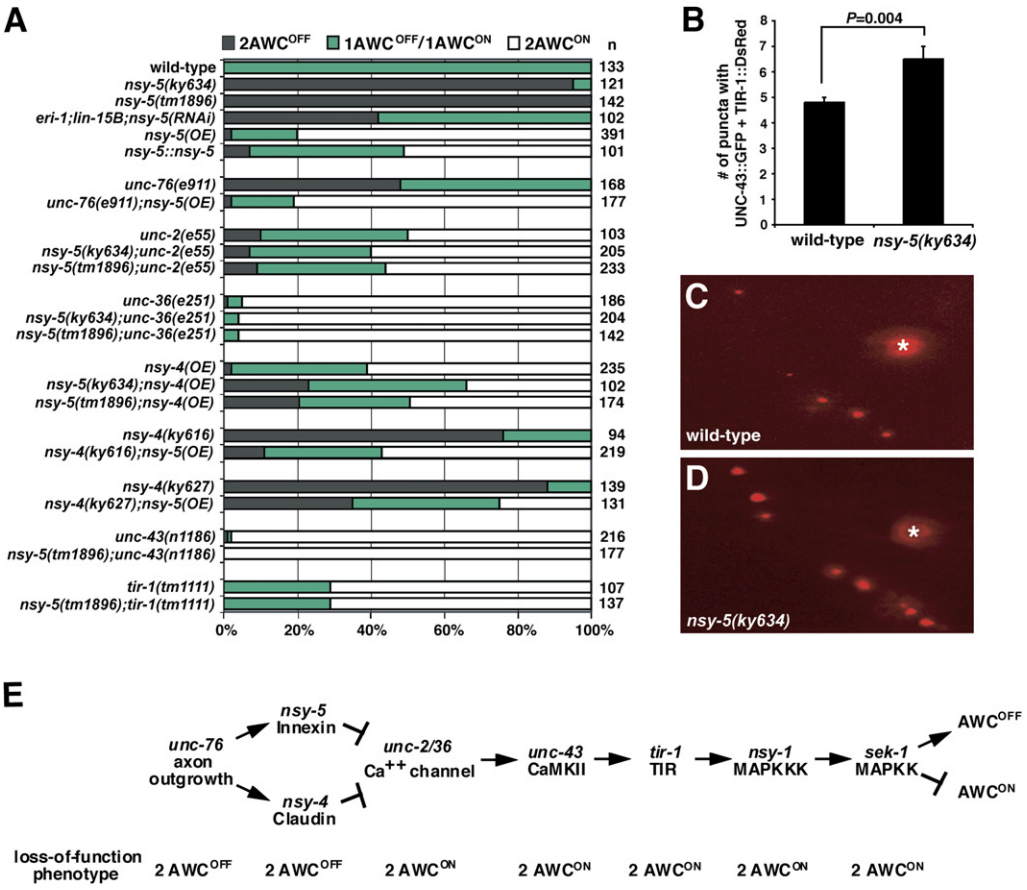

Figure 2. *nsy-5* Antagonizes Calcium and Kinase Signaling

(A) AWC phenotypes in single and double mutants. RNA interference of *nsy-5* was performed in the RNAi-sensitive strain *eri-1(mg366);lin-15B(n744)* double mutant as described (Kamath et al., 2001; Sieburth et al., 2005). *nsy-5(OE)* overexpresses the *nsy-5* genomic region and corresponds to line 4 in Figure 6D. *nsy-5::nsy-5* is a *nsy-5a* cDNA expressed from the 5.8 kb *nsy-5* promoter. *nsy-4(OE)* overexpresses *nsy-4* from the *odr-3* promoter. For *unc-76*, *unc-2*, *unc-36*, and *unc-43*, strong alleles that appear to be molecular null alleles were used. For *nsy-4* and *tir-1*, the strongest available reduction-of-function alleles were used.

(B) Number of colocalized UNC-43::GFP and TIR-1::DsRed puncta in wild-type and *nsy-5(ky634)* AWC axons. Error bars indicate standard error of the mean.

(C and D) *odr-3::tir-1::DsRed* expression in wild-type and *nsy-5(ky634)* animals showing synaptic puncta in AWC axons. Asterisks indicate cell body.

(E) One possible model for relationships between *nsy* mutants. *nsy-5* may act together with *nsy-4*, upstream of or parallel to *unc-2*/*unc-36*.

proteins with alternative N termini derived from alternative promoters (www.wormbase.org) (Figures 1F and 1G). Like other innexin proteins, NSY-5 is predicted to have four transmembrane domains and intracellular N and C termini (Figure 1F). There are 25 predicted innexin/pannexin-encoding genes in *C. elegans*, 8 in *Drosophila melanogaster*, and 3 in the human genome (Phelan, 2005; Starich et al., 2001; Stebbings et al., 2002). In *C. elegans*, innexins have physiological roles as gap junctions in neurons, pharyngeal muscles, and body-wall muscles (Li et al., 2003; Liu et al., 2006; Starich et al., 1996). Innexins affect the formation of neuronal and nonneuronal gap junctions in *C. elegans* and *Drosophila* and can form gap junctions when expressed in heterologous cells (Bauer et al., 2004; Curtin et al., 2002; Starich et al., 1996; Landesman et al., 1999; Phelan et al., 1998; Stebbings et al., 2000). Although most vertebrate gap junctions are formed by the unrelated connexin family, the human pannexin (innexin-like) proteins also form gap junctions (Bruzzone et al., 2003).

The *nsy-5(ky634)* allele was associated with a G→A point mutation, resulting in a predicted glutamic-acid-to-lysine change in the second exon of both T16H5.1 isoforms (Figures 1F and 1G). *nsy-5(tm1896)*, an in-frame deletion in the third and fourth exons of both T16H5.1 isoforms (generously provided by S. Mitani), caused a strong 2 AWC^{OFF} phenotype, as did RNA interference of the T16H5.1 gene (Figure 1C; Figure 2A). These results suggest that *nsy-5(ky634)* and *nsy-5(tm1896)* are loss-of-function alleles of T16H5.1 and that reduction of *nsy-5* function leads to a 2 AWC^{OFF} phenotype.

Overexpression of a genomic *nsy-5* fragment in a wild-type background generated a 2 AWC^{ON} phenotype

Genetic Background	Row #	Transgene	2AWC^{OFF} (%)	1AWC^{OFF}/1AWC^{ON} (%)	2AWC^{ON} (%)	n	Cells with *nsy-5* activity AWC	ASH	AFD	AWB
nsy-5(ky634)		none	95	5	0	121	-	-	-	-
		nsy-5(genomic)#1	8	46	46	487	+	+	+	+
	1	*nsy-5(genomic)#2*	10	85	5	353	+	+	+	+
		nsy-5(genomic)#3	10	57	33	451	+	+	+	+
	2	*nsy-5::nsy-5::DsRed*	7	63	30	74	+	+	+	+
	3	*nsy-5::nsy-5b::DsRed*	3	39	58	168	+	+	+	+
	4	*nsy-5::nsy-5*	4	47	49	120	+	+	+	+
	5	*odr-3::nsy-5#1*	26	54	20	155	+	-	-	+
		odr-3::nsy-5#2	23	43	33	129	+	-	-	+
	6	*tax-4::nsy-5*	33	66	1	103	+	-	+	-
	7	*sra-6::nsy-5*	98	2	0	108	-	+	-	-
	8	*gcy-8::nsy-5*	97	3	0	106	-	-	+	-
	9	*str-1::nsy-5*	100	0	0	63	-	-	-	+
	10	*odr-3::nsy-5; str-1::nsy-5*	41	48	11	143	+	-	-	+
	11	*odr-3::nsy-5; gcy-8::nsy-5*	43	54	3	100	+	-	+	+
	12	*sra-6::nsy-5; gcy-8::nsy-5*	95	5	0	107	-	+	+	-
	13	*odr-3::nsy-5; sra-6::nsy-5*	5	26	69	137	+	+	-	-
	14	*sra-6::nsy-5; tax-4::nsy-5*	21	79	0	67	+	+	+	-
	15	*odr-3::nsy-5; sra-6::nsy-5; tax-4::nsy-5*	20	77	3	75	+	+	+	-
	16	*odr-3::nsy-5; sra-6::nsy-5; gcy-8::nsy-5*	74	24	2	171	+	+	+	-
Wild-type		none	0	100	0	133	+	+	+	+
	17	*nsy-5(genomic)#1*	4	36	60	325	++	++	++	++
		nsy-5(genomic)#4	2	18	80	391	++	++	++	++
	18	*nsy-5::nsy-5*	7	42	51	101	++	++	++	++
	19	*odr-3::nsy-5*	5	92	3	109	++	+	+	++
	20	*tax-4::nsy-5*	4	95	1	121	++	+	++	+
	21	*sra-6::nsy-5*	0	100	0	128	+	++	+	+
	22	*gcy-8::nsy-5*	0	100	0	119	+	+	++	+
	23	*str-1::nsy-5*	1	99	0	82	+	+	+	++
	24	*odr-3::nsy-5; str-1::nsy-5*	7	86	7	113	++	+	+	++
	25	*str-1::nsy-5; gcy-8::nsy-5*	0	100	0	197	+	+	++	++
	26	*sra-6::nsy-5; gcy-8::nsy-5*	0	100	0	132	+	++	++	+
	27	*odr-3::nsy-5; sra-6::nsy-5*	3	37	60	185	++	++	+	+
	28	*sra-6::nsy-5; tax-4::nsy-5*	2	96	2	183	++	++	++	+
	29	*odr-3::nsy-5; sra-6::nsy-5; tax-4::nsy-5*	8	86	6	101	++	++	++	+
	30	*odr-3::nsy-5; sra-6::nsy-5; gcy-8::nsy-5*	4	84	12	109	++	++	++	+
	31	*odr-3::nsy-5; sra-6::nsy-5; str-1::nsy-5*	10	85	5	242	++	++	+	++

Figure 3. Expression of *nsy-5* in Different Cells

All transgenes except *nsy-5(genomic)* and *nsy-5::nsy-5b::DsRed* express *nsy-5a cDNA* and include the *nsy-5* 3′ region (1117 bp) at the end of *nsy-5a* cDNA. Each result was combined from three to five transgenic lines that showed similar penetrance of phenotypes. Orange indicates *nsy-5* activity in AWC. Green indicates *nsy-5* activity in AFD or AWB that reduced the rescuing activity of *odr-3::nsy-5*. Red indicates *nsy-5* activity in ASH that resulted in a cooperative interaction with AWC. Blue indicates *nsy-5* activity in AFD or AWB that antagonized the cooperative interaction between AWC and ASH. Colored values are statistically different from controls at $p < 0.05$ by comparison of two proportions with Bonferroni correction. Control for data in orange = no transgene; control for data in green or red = *odr-3::nsy-5* transgene; control for data in blue = *[odr-3::nsy-5, sra-6::nsy-5]* transgene.

opposite to the *nsy-5* loss-of-function phenotype (Figure 2A; Figure 3, row 17). Transgenes expressing either alternative transcript of T16H5.1 as a cDNA also rescued *nsy-5* mutants and caused a gain-of-function phenotype (Figure 2A; Figure 3, rows 2–4 and 18). These results indicate that the level of *nsy-5* activity can specify AWC asymmetry in an instructive manner, with a low level of *nsy-5* activity defining the AWC^{OFF} state and a high level of activity defining the AWC^{ON} state.

nsy-5 Antagonizes *unc-2*/*unc-36* Calcium Signaling

The relationship between *nsy-5* and other genes affecting AWC asymmetry was characterized by analyzing double mutants (Figure 2A). The 2 AWC^{OFF} phenotype of *nsy-5* mutants was suppressed by mutations in the calcium-channel genes *unc-2* (α1 subunit) and *unc-36* ($\alpha 2\delta$ subunit) and by mutations in the downstream kinase pathway: *unc-43* (CaMKII), *tir-1* (SARM/adaptor protein), and *nsy-1* (ASK1/MAPKKK). These results suggest that *nsy-5* acts upstream of the calcium signaling pathway. The 2 AWC^{OFF} phenotype of the axon guidance mutant *unc-76* was suppressed in *unc-76(lf);nsy-5(OE)* double mutants, suggesting that *nsy-5* activity does not require the signal provided by axon guidance.

Like *nsy-5*, the claudin/calcium channel γ subunit *nsy-4* antagonizes *unc-2* and *unc-36* by acting either upstream of or parallel to the calcium-channel pathway (VanHoven et al., 2006). Both *nsy-5(OE) nsy-4(lf)* and *nsy-5(lf) nsy-4(OE)* double mutants had a mixed phenotype compared to single mutants, suggesting that *nsy-4* and *nsy-5* act in parallel, with each having some activity in the absence of the other. This interpretation is tentative because the strongest *nsy-4* mutation causes substantial lethality and may not be a null allele, and null alleles might in principle be fully epistatic to *nsy-5.* With that qualification, one possible model is that both *nsy-4* and *nsy-5* inhibit the calcium-channel pathway during AWC signaling (Figure 2E).

The downstream AWC signaling proteins UNC-43(CaMKII) and TIR-1 reside together at postsynaptic regions of AWC axons (Chuang and Bargmann, 2005; Rongo and Kaplan, 1999). Although both wild-type and *nsy-5(lf)* animals had UNC-43^{+}TIR-1^{+} puncta in their AWC axons, the numbers of puncta were significantly different. Wild-type animals had an average of 4.7 UNC-43^{+}TIR-1^{+} puncta per animal (n = 16), whereas *nsy-5(lf)* animals had 6.5 puncta per animal (n = 11) (Figures 2B–2D). These results are consistent with an inhibitory relationship between *nsy-5* and the UNC-43/MAPK pathway. No molecular interaction was evident between *nsy-4* and *nsy-5*: the expression and localization of tagged NSY-4::GFP were unaltered in *nsy-5* mutants, and the expression and localization of NSY-5::GFP were unaltered in *nsy-4* mutants (data not shown).

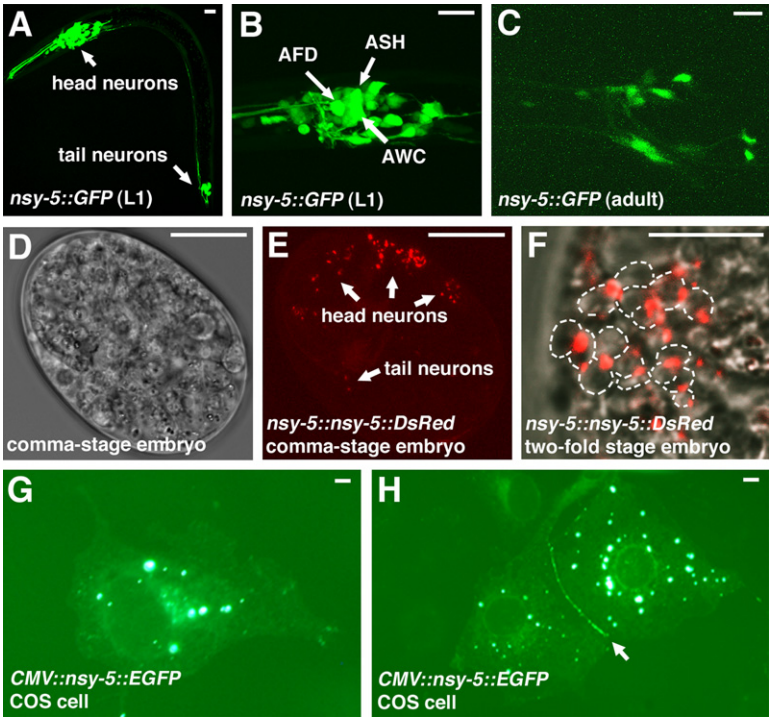

Figure 4. Expression of NSY-5 Reporter Genes

(A–C) Expression of *nsy-5::GFP* promoter fusion.

(A) L1 animal.

(B) Higher magnification of L1 head neurons.

(C) Adult animal.

(D–F) Subcellular localization of tagged NSY-5::DsRed. DIC and confocal projections of comma-stage embryos (D and E) and 2-fold-stage embryos (F) expressing *nsy-5::nsy-5::DsRed* false-colored red are shown.

(G and H) Subcellular localization of tagged NSY-5::EGFP in an isolated COS cell (G) and in two adjacent COS cells (H). Arrow indicates the cell-cell contact region. Scale bar = 10 μm in all panels.

NSY-5 Is Localized to Cell Bodies in AWC and Adjacent Neurons

A GFP reporter transgene with 5.8 kb of the *nsy-5* promoter was expressed exclusively in sensory neurons and interneurons in the head and tail (Figures 4A and 4B). The neurons that expressed *nsy-5::GFP* included AWC, ASH, AFD, ASI, ADL, ASK, BAG, AWB, and ADF (head sensory neurons); ADA, AIZ, RIC, AIY, and AIM (head interneurons); PHA and PHB (tail sensory neurons); and PVC and PVQ (tail interneurons). Expression began about halfway through embryogenesis, was strongest in late embryogenesis and the L1 larval stage, and faded thereafter. Adults maintained weak expression in several neurons, including ASH but not AWC (Figure 4C).

Tagged NSY-5::GFP and NSY-5::DsRed fusion proteins that rescued *nsy-5* mutants were first detected in embryos in a punctate pattern surrounding the sensory neurons and interneurons that expressed *nsy-5::GFP* (Figure 3; Figures 4D–4F; data not shown). Individual NSY-5 puncta appeared to reside at the borders between neuronal cell bodies (Figure 4F) and were largely excluded from axons and dendrites.

The subcellular localization of NSY-5 was examined in COS cells expressing a heterologous NSY-5::EGFP fusion protein. In isolated COS cells, NSY-5::EGFP was observed mainly in intracellular vesicles (Figure 4G). In pairs of COS cells that contacted each other, NSY-5::EGFP clustered at points of cell-cell contact, but only when both cells expressed NSY-5 (Figure 4H). These results suggest that NSY-5 forms homophilic complexes at the plasma membranes of adjacent cells, like other gap-junction proteins.

NSY-5 Forms a Gap-Junction Network Linking Embryonic Neurons

The expression of an innexin gene in AWC was surprising since AWC gap junctions do not appear in the anatomical reconstruction of the adult *C. elegans* nervous system (White et al., 1986). The early expression of *nsy-5* reporter genes presented a possible resolution for this discrepancy. To search for gap junctions associated with immature AWC neurons, we performed serial-section electron microscopy and examined the AWC neurons of wild-type embryos between 7 and 12 hr after fertilization, the time at which *nsy-5* reporter genes are most highly expressed, and from an L1 larva. We found that embryonic AWC neurons and many other nerve-ring neurons had extensive junctions connecting their cell bodies (Figure 5A). High-resolution analysis of these junctions in the *nsy-5*-expressing cells AWC, ASH, and AFD revealed that the AWC-ASH and ASH-AFD junctions had the pentalamellar structure, ~2 nm electron-dense extracellular gap, and 15–16 nm junctional width characteristic of gap junctions in *C. elegans* and other animals (Figures 5B and 5D; see also Table S1 in the Supplemental Data available with this article online) (Starich et al., 2003; Zampighi et al., 1980). Their ultrastructural features were distinct from those of adherens junctions and desmosomes in the same embryos (Figure S1). These results suggest that AWC and neighboring neurons are linked by gap junctions in wild-type embryos.

In the wild-type L1 animal, junctions between AWC, ASH, and AFD lacked the pentalamellar electron-dense structure, and the cells became less tightly associated, with an 18–20 nm junctional width (Figure 5C; Table

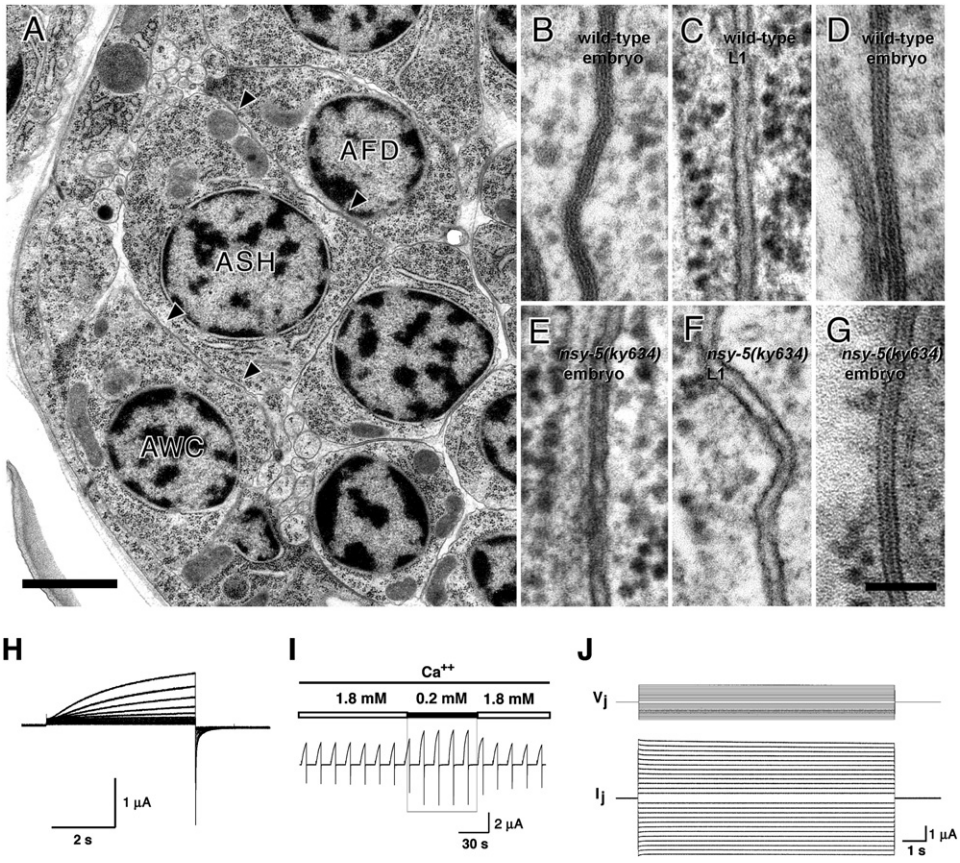

Figure 5. *nsy-5* Forms Embryonic Junctions, Hemichannels, and Gap-Junction Channels

(A–G) Electron micrographs of intercellular junctions.

(A) Cell bodies of neurons in wild-type embryos. Linear regions between two arrowheads are potential gap junctions. Scale bar = 1 μm.

(B, C, E, and F) Intercellular junctions between the AWC cell body and adjacent neuron in wild-type embryo (B), wild-type L1 (C), *nsy-5(ky634)* embryo (E), and *nsy-5(ky634)* L1 (F). Scale bar = 50 nm in (B–G).

(D and G) Gap junctions between hypodermal cells and excretory cells in wild-type (D) and *nsy-5(ky634)* embryos (G), which resemble the intercellular junction shown in (B). Measurements of intercellular junctions are provided in Table S1.

(H) Recordings of membrane currents in single *Xenopus* oocytes expressing *nsy-5*. From a holding potential of −70 mV, voltage steps from −100 to +50 mV were applied in increments of +10 mV. Slowly activating outward currents were observed upon depolarization to positive voltages.

(I) Recordings of NSY-5 hemichannel currents in response to repeated voltage steps to +40 mV applied from a holding potential of −70 mV. Lowering external Ca^{2+} from 1.8 mM to 0.2 mM (boxed region) resulted in a reversible increase in current magnitude.

(J) Junctional currents (I_j) between a pair of *Xenopus* oocytes in response to a series of transjunctional voltage (V_j) steps were recorded using a dual two-electrode voltage-clamp configuration. Cells were clamped to a common holding potential of −30 mV, and hyperpolarizing and depolarizing voltages from −120 to +120 mV were applied to one cell in 10 mV increments. Currents showed little decline with voltage. Uninjected oocyte controls are shown in Figure S3.

S1A). These observations suggest that AWC junctions are dissolved or remodeled in the L1 stage. Gap junctions were not observed at the cell bodies of the AWC neurons in adult sections from the White series (White et al., 1986 and data not shown).

To ask whether the AWC junctions were formed by NSY-5 innexins, we fixed and sectioned two *nsy-5(ky634)* embryos at the 3-fold-to-pretzel stage and a *nsy-5(ky634)* L1 larva. In *nsy-5* embryos, no pentalamellar electron-dense structure was observed between AWC-ASH or ASH-AFD (Figure 5E), and the distance between these cells was increased to 17.8–18.8 nm (Table S1A). In the same *nsy-5(ky634)* embryos, the gap junctions between excretory cells and hypodermal cells were intact, indicating that gap junctions were not destroyed by poor fixation (Figure 5G; Table S1B). The *nsy-5* L1 animal also lacked AWC gap junctions (Figure 5F; Table S1A). These results suggest that NSY-5 functions as a gap-junction protein to establish transient embryonic connections between the cell bodies of AWC and adjacent neurons.

The *nsy-5*-expressing neurons ASK and ADL belong to left-right pairs that are close to each other at the dorsal midline (White et al., 1986), raising the possibility that the *nsy-5*-dependent junctions might directly link left and right clusters of neuronal cell bodies. We examined the entire contact regions for ASK and ADL neurons in two wild-type

embryos. In all sections, the cell bodies of the left and right neuron were clearly separated by an extracellular matrix layer at least 15 nm thick, and no gap junctions were observed between the left and right sides (Figure S2).

NSY-5 Forms Functional Hemichannels and Gap-Junction Channels

To determine directly whether NSY-5 can form gap-junction channels, we expressed it in *Xenopus* oocytes. In single oocytes injected with NSY-5 mRNA, slowly activating outward currents were induced by depolarizing steps to positive voltages (Figure 5H; Figure S3). This result suggests that NSY-5 forms functional hemichannels. As seen for connexin hemichannels (Ebihara and Steiner, 1993; Saez et al., 2005), reduction of extracellular calcium promoted opening of NSY-5 hemichannels (Figure 5I).

To determine whether NSY-5 can induce the formation of intercellular channels, two RNA-injected oocytes with their vitelline membrane removed were brought into contact. After 24 hr, electrical coupling was detected using the dual two-electrode voltage-clamp technique (Figure 5J; Figure S3). NSY-5 expression resulted in electrical coupling and currents that showed little decline with transjunctional voltage steps, suggesting that they are voltage independent or only weakly voltage dependent. (Endogenous oocyte currents, which were suppressed by injecting antisense oligonucleotides to *XenCx38*, are strongly voltage dependent.) These results suggest that NSY-5 can function both as intercellular channels and as hemichannels.

nsy-5 Acts in a Network of Cells to Promote or Inhibit AWC Signaling

The site of *nsy-5* action was examined using three different types of experiments. First, we expressed *nsy-5* cDNAs under different promoters in *nsy-5* mutant and wild-type backgrounds (Figure 3). Second, we performed genetic mosaic analysis on animals expressing a genomic *nsy-5* fragment that should mimic the endogenous *nsy-5* expression pattern (Figure 6). Third, combining directed expression and mosaic analysis, we examined the effect of expressing *nsy-5* only in a single AWC neuron (Figure 6G).

For targeted expression of *nsy-5*, we used promoters that overlapped with the *nsy-5* expression pattern in AWC and AWB (*odr-3*); AWB (*str-1*); AFD (*gcy-8*); ASH, ASI, and PVQ (*sra-6*; due to its proximity to AWC, ASH is likely to be the relevant cell); and AWC, AWB, AFD, ASK, and ASI (*tax-4*). Only transgenes expressed in AWC neurons were able to rescue *nsy-5* mutants, suggesting that one important site of *nsy-5* action is AWC (Figure 3, rows 4–9). However, expression of *nsy-5* in other neurons modified the rescue in AWC neurons. Simultaneous *nsy-5* expression from *odr-3* (AWC) and *sra-6* (ASH) promoters led to a strong gain-of-function 2 AWC^{ON} phenotype not observed with either promoter alone (Figure 3, row 13). This enhancement was suppressed when *nsy-5* was simultaneously expressed from *odr-3* (AWC), *sra-6* (ASH), and *gcy-8* (AFD) promoters (Figure 3, row 16). These results suggest that the ultrastructural AWC-ASH and ASH-AFD gap junctions are functionally significant and that ASH and AFD neurons have opposite effects on AWC: *nsy-5* in ASH favors the AWC^{ON} state, whereas *nsy-5* in AFD favors the AWC^{OFF} state (see below).

The AWC-ASH-AFD interaction was also observed when *nsy-5* transgenes were expressed in a wild-type background. At the low DNA concentrations used to make these transgenic lines, no appreciable gain-of-function phenotypes were generated by introducing individual transgenes into wild-type strains (Figure 3, rows 19–23). However, expression of *nsy-5* in both AWC and ASH generated a strong 2 AWC^{ON} gain-of-function phenotype (Figure 3, row 27) that was suppressed by coexpression of *nsy-5* in AFD or AWB (Figure 3, rows 30 and 31). These results suggest that AFD and AWB antagonize a cooperative interaction between AWC and ASH even when the complete normal complement of *nsy-5*-expressing cells is present.

nsy-5 Acts Cell Autonomously in the Future AWC^{ON} Neuron and in Other Cells

To further refine the site of *nsy-5* action, mosaic animals in which *nsy-5* activity differed between the two AWC neurons were used to ask whether *nsy-5* acts in the future AWC^{ON} cell, the future AWC^{OFF} cell, or both. Mosaic animals were generated by random loss of an unstable transgene with the *nsy-5* genomic clone and an *odr-1*::*DsRed* marker (expressed in AWC and AWB) that showed which cells retained the transgenic array.

Transgenes expressing the *odr-1::DsRed* marker in both AWC neurons rescued *nsy-5(lf)* mutants, resulting in a mixture of 1 AWC^{ON} and 2 AWC^{ON} animals (Figure 3, row 1; Figure 6A). Spontaneous loss of the extrachromosomal array resulted in mosaic animals in which one of the two AWC neurons expressed DsRed fluorescence and *nsy-5* activity. In the majority of these mosaic animals, the *nsy-5*$^{+}$ AWC neuron expressed *str-2::GFP* and the *nsy-5*- AWC neuron did not (Figures 6A, 6B, and 6E). These results are consistent with a significant cell-autonomous requirement for *nsy-5* within the future AWC^{ON} neuron. Mosaic analysis was also conducted in transgenic lines in which *nsy-5* was overexpressed in a wild-type background, resulting in a 2 AWC^{ON} phenotype (Figure 3, row 17; Figure 6C). When the transgene was retained in only one of the AWC neurons, the *nsy-5(OE)* neuron expressed *str-2::GFP* over 80% of the time (Figures 6C and 6D), suggesting that *nsy-5* has a cell-autonomous ability to promote the AWC^{ON} receptor choice. The DsRed-negative AWC neuron in these mosaic animals, which should have a wild-type genotype, nearly always became AWC^{OFF}. This result suggests that the decision of one AWC neuron to become AWC^{ON} due to *nsy-5* overexpression was sensed by the wild-type AWC neuron, which then became AWC^{OFF}.

The invariant cell lineage of *C. elegans* can be used to infer the genotype of cells in mosaic animals (Figure 6F), providing an additional route to identify cells that affect

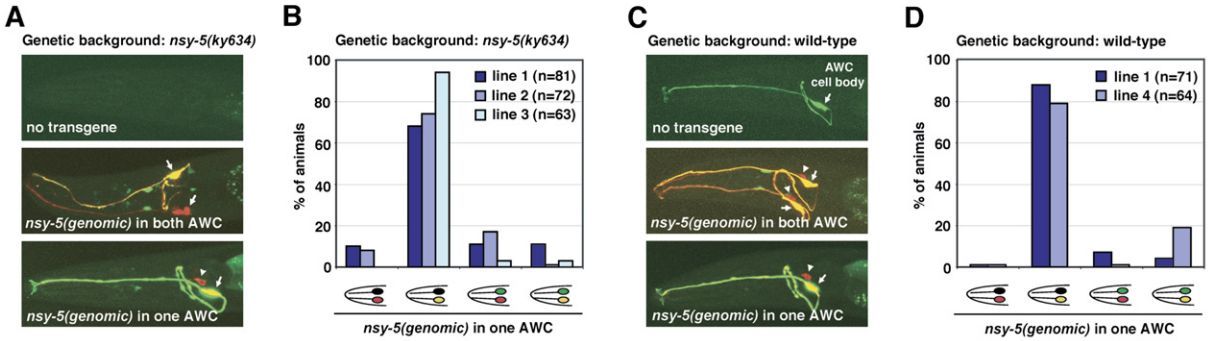

F

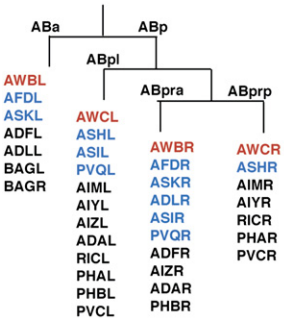

G

Genetic background	Array	Inferred loss	Row	Array present in				Phenotype (%)				
				AWBL	AWCL	AWBR	AWCR	2AWC^{OFF}	AWCL^{ON}	AWCR^{ON}	2AWC^{ON}	n
nsy-5(ky634)	*nsy-5(genomic)#2*	None	a	+	+	+	+	9	41	45	5	132
		ABpl	b	+	-	+	+	5	19	76	0	21
		ABprp	c	+	+	+	-	7	76	17	0	29
		ABpr	d	+	+	-	-	7	60	33	0	15
		ABpra	e	+	+	-	+	2	26	71	1	89
		ABa, pl	f	-	-	+	+	0	43	57	0	7
		ABpl, pra	g	+	-	-	+	7	21	71	0	14
		ABa, pr	h	-	+	-	-	0	57	43	0	7
		ABa, pl, pra	i	-	-	-	+	0	25	75	0	12
wild-type	*nsy-5(genomic)#4*	None	j	+	+	+	+	4	27	21	49	181
		ABpl	k	+	-	+	+	10	1	76	13	69
		ABprp	l	+	+	+	-	11	78	6	5	36
		ABpl,prp	m	+	-	+	-	83	9	8	0	23
nsy-5(ky634)	*odr-3::nsy-5*	None	n	+	+	+	+	18	15	19	48	297
		ABa,pr	o	-	+	-	-	86	14	0	0	29
		ABa, pl,pra	p	-	-	-	+	7	0	93	0	15
		ABprp	q	+	+	+	-	20	80	0	0	10
		ABpl	r	+	-	+	+	62	0	38	0	13
nsy-4(ky616)	*odr-3::nsy-4*	ABa,pr	s	-	+	-	-	19	78	3	0	32
		ABa, pl,pra	t	-	-	-	+	47	6	47	0	36
		ABprp	u	+	+	+	-	45	55	0	0	40
		ABpl	v	+	-	+	+	43	0	57	0	46

Figure 6. *nsy-5* Functions in Multiple Lineages to Affect AWC Asymmetry

(A and C) Confocal projections of *nsy-5(ky634)* (A) and wild-type (C) animals with an integrated *str-2::GFP* transgene and an unstable transgenic array bearing *nsy-5* genomic sequence and *odr-1::DsRed*. AWC neurons that express both GFP and DsRed appear yellow. Arrows, AWC cell body; arrowhead, AWB cell body. Anterior is at left; ventral is down.

(B and D) Phenotypes of *nsy-5(ky634)* (B) and wild-type (D) mosaic animals expressing *[nsy-5(genomic), odr-1::DsRed]* transgenes in one AWC neuron.

(E) Color codes for AWC neurons in (B) and (D).

(F) Simplified cell lineage of *C. elegans* starting at the second cell division, with origin of *nsy-5::GFP*-expressing cells. Cells traced by *odr-1::DsRed* expression in mosaic analysis are indicated in red. Additional cells tested for rescue using cell-specific transgenes (Figure 3) are indicated in blue.

(G) Genetic mosaic analysis of animals expressing a *nsy-5* genomic clone under its own promoter, *odr-3::nsy-5*, or *odr-3::nsy-4*. The percentage of animals with each phenotype is indicated; n = number of mosaic animals characterized. Red data in rows a–m indicate mosaic classes inconsistent with a pure model in which *nsy-5* acts only in AWC cell autonomously (positively) and nonautonomously (negatively). Values in red are different from the pure model at $p < 0.05$. Asterisks in rows n–v indicate comparisons that are different at $p < 0.01$. Statistical comparisons were made by chi-square test or Fisher's exact test as appropriate.

AWC signaling. The ASH neurons are very closely related to the ipsilateral AWC neuron by lineage, but many other neurons that express *nsy-5* are closely related to the ipsilateral AWB, allowing their genotypes to be inferred by following the *odr-1::DsRed* marker in AWB (Figure 6F). For the most part, mosaic analysis following both AWB and AWC lineages suggested that the important site of *nsy-5* expression was the lineage that produced ASH and AWC, a result consistent with the targeted expression experiments (Figure 3; Table S2). However, several classes of mosaic animals indicated that *nsy-5* rescue is not entirely cell autonomous to AWC^{ON}. First, in a minor but significant class of mosaic animals, a *nsy-5* mutant AWC neuron became AWC^{ON}, suggesting nonautonomous rescue of AWC (Figure 6G, rows b–d and f–i). Second, mosaic animals that lost the array in the AWBR lineage (ABpra) but retained it in both AWC neurons had a significant bias in left-right asymmetry, such that 71% of the AWCR neurons became AWC^{ON} (Figure 6G, row e). This result suggests that *nsy-5*-expressing cells in the ABpra lineage affect communication between the two AWC neurons.

The effect of the *nsy-5*-overexpressing transgene in the wild-type background was largely dependent on the genotype of the AWC neurons (Figure 6G, rows j–l; Table S2). However, a rare class of mosaics in which *nsy-5* was overexpressed in both AWB lineages but not in either AWC had an unexpected 2 AWC^{OFF} loss-of-function phenotype (Figure 6G, row m). These mosaics indicate that overexpression of *nsy-5* in cells related to AWB can cause a dominant disruptive effect on AWC signaling. In total, the mosaic results strengthen the conclusion that a network of cells communicates with AWC in *nsy-5*-dependent signaling.

nsy-4 and *nsy-5* Have Opposite Side Biases in AWC

NSY-5 can form either intracellular hemichannels or intercellular gap-junction channels in oocytes (Figure 5). To determine whether hemichannels could contribute to *nsy-5* activity, we wished to express *nsy-5* only in a single AWC neuron. As the endogenous *nsy-5* promoter is expressed in many cells, we achieved restricted expression by performing *nsy-5* mosaic analysis with *odr-3::nsy-5* transgenes, which are consistently expressed only in AWC and AWB neurons (Figure 6G). When *odr-3::nsy-5* was retained only in AWCR and in neither AWB, over 90% of AWCR neurons became AWC^{ON} (Figure 6G, row p), a result suggesting that AWCR might respond to NSY-5 on its own. However, when *odr-3::nsy-5* was retained only in AWCL, only 14% of the AWCL neurons became AWC^{ON} (Figure 6G, row o). Expression of *odr-3::nsy-5* in AWCL, AWBL, and AWBR allowed AWCL neurons to become AWC^{ON} (Figure 6G, row q). These experiments reveal an unexpected asymmetry between AWCL and AWCR in their response to *nsy-5*.

Like *nsy-5*, the claudin-like gene *nsy-4* has both autonomous and nonautonomous effects on AWC asymmetry (VanHoven et al., 2006). To determine whether *nsy-4* activity in AWC has a bias for rescue like *nsy-5*, we analyzed *odr-3::nsy-4;odr-1::DsRed* mosaics analogous to those examined for *nsy-5*. A significant bias was observed, but unlike *nsy-5*, *nsy-4* in a single cell rescued AWCL more efficiently than AWCR (Figure 6G, rows s and t).

DISCUSSION

The innexin gap-junction protein NSY-5, a component of the AWC signaling pathway, is localized to the cell bodies of a subset of neurons including AWC. These neighboring neurons form transient, *nsy-5*-dependent junctions in embryos that are required for the asymmetric differentiation of the two AWC neurons. Although we have not demonstrated electrical communication through *nsy-5* junctions in vivo, electrical recordings from *Xenopus* oocytes injected with *nsy-5* RNA indicate that NSY-5 can form both hemichannels and intercellular gap-junction channels.

The analysis of *nsy-5* uncovered an unanticipated network of neurons that regulates left-right asymmetry of AWC. A model for *nsy-5* function in this network is presented in Figure 7. We propose that NSY-5 gap junctions and NSY-4 claudins represent parallel signaling systems that act together to induce the AWC^{ON} state. Based on an intrinsic bias, AWCR is preferentially sensitive to *nsy-5* activity and AWCL is more sensitive to *nsy-4*. These two subthreshold signals can cooperate when the left and right axons meet in the nerve ring, pushing the interacting cells above a threshold for AWC^{ON} induction. After induction, feedback from the most strongly induced AWC neuron drives the contralateral AWC neuron to become AWC^{OFF}. The evidence for this model is discussed below.

Parallel Functions

Both *nsy-4* and *nsy-5* are required for AWC^{ON} induction in wild-type animals, but overexpression of either gene allows AWC^{ON} induction when the other gene is mutant. These results are consistent with parallel activity in which either gene can promote AWC^{ON} induction, although not definitive because the strongest *nsy-4* allele is nonnull. However, a parallel model is also favored by the dissimilar expression of *nsy-4* and *nsy-5*. Reporter genes to *nsy-4* and *nsy-5* are largely nonoverlapping outside AWC: *nsy-4* is expressed in epithelial cells and excretory cells, whereas *nsy-5* is exclusively neuronal. Within AWC, NSY-4 is ubiquitous at the plasma membrane, while NSY-5 resides in puncta at cell junctions. The only apparent overlap between these genes occurs in AWC^{ON} induction.

Intrinsic Bias

Despite the random left-right differentiation of AWC^{ON}, the detailed analysis of mosaic animals suggests that the left and right AWC neurons are different in their potential to respond to *nsy-5*. AWCR can respond to *nsy-5* efficiently even when it is predicted to be the only *nsy-5*-expressing cell in the animal, but AWCL cannot. AWCR may be preferentially sensitive to the hemichannel activity of NSY-5 due to intrinsic properties or signals from nearby cells. Alternatively, NSY-5 in AWCR may be capable of interacting with other innexins expressed on the right side of the animal (Starich et al., 2001) (http://elegans.bcgsc.ca/home/sage.html).

In contrast with *nsy-5*, *nsy-4* appears to rescue AWCL more efficiently than AWCR. The *nsy-4* and *nsy-5* experiments were designed to be parallel controls for one another: both sets of transgenes were generated with the same *odr-3* promoter and coinjection markers and similar DNA concentrations. In addition, control plasmids with frameshift mutations in the coding regions of either *nsy-4* and *nsy-5* cDNAs did not have biological activity, and parallel mosaic experiments with other genes such as *unc-43*, *tir-1*, and *nsy-1* did not show these effects (Chuang and Bargmann, 2005; Sagasti et al., 2001; VanHoven et al., 2006). Therefore, these results are best explained by an underlying difference between AWCL and AWCR.

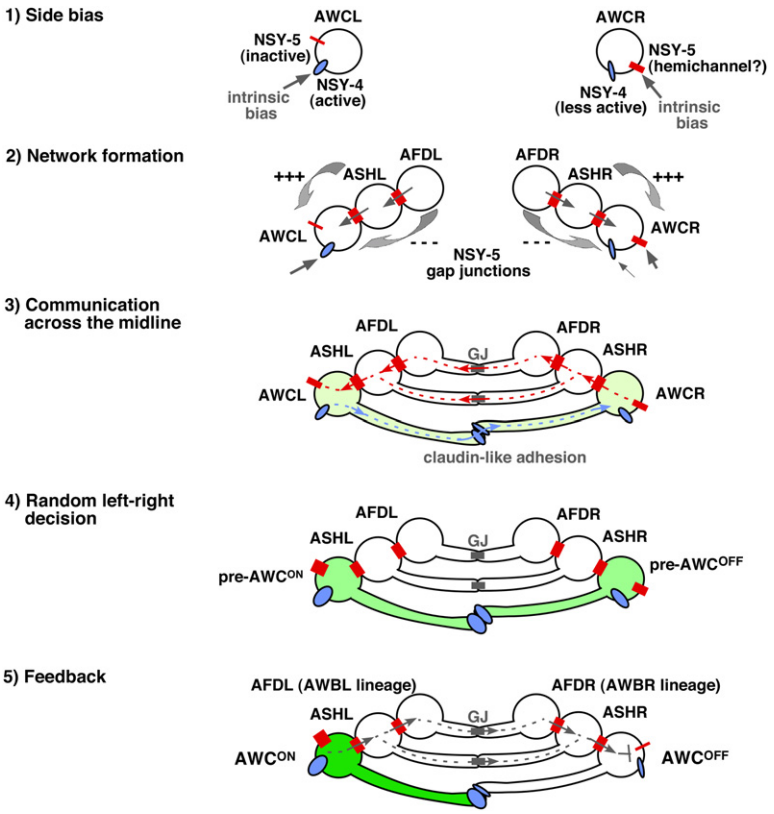

Figure 7. Model for the Asymmetric AWC Signaling Network

An intrinsic bias makes AWCR more sensitive to *nsy-5* than AWCL. Network formation and communication across the midline allow cooperation between subthreshold *nsy-5* and *nsy-4* signals for induction of AWC^{ON}. Feedback from the more strongly induced cell causes the contralateral cell to become AWC^{OFF}. GJs (gray) are gap junctions known from adult reconstructions (White et al., 1986). See Discussion for details.

Network Formation

The state of *nsy-5* activity in non-AWC neurons can promote either the AWC^{ON} or the AWC^{OFF} state; together with the ultrastructural data, these results support the proposal that *nsy-5*-expressing cells form a gap-junction network. Genetic mosaic analysis suggests contributions from cell lineages related to AWB, and targeted expression suggests contributions from ASH, AFD, and AWB. AWC and ASH are linked by morphological gap junctions, and targeted expression suggests that these two cells can cooperate to promote the AWC^{ON} state. ASH and AFD are linked by gap junctions, but AWC and AFD are not, and AFD appears to inhibit the AWC^{ON} state indirectly—it only affects AWC when AWC, ASH, and AFD all express *nsy-5.*

Communication across the Midline

An intriguing aspect of AWC asymmetry is the coordination between left and right AWC neurons that are distant from each other. Since axon guidance mutants are defective in AWC signaling, we propose that left-right communication occurs when axons from the left and right sides meet, allowing them to propagate the subthreshold *nsy-4* and *nsy-5* signals across the midline. Under normal circumstances, the cooperation of these two signals results in sufficient signaling to induce the AWC^{ON} state in either neuron.

In the mature nervous system, many neuron pairs including ASH, AFD, and AWB are connected by axonal gap junctions at the midline, but AWC neurons are not (White et al., 1986). It is possible that the subthreshold *nsy-5* signal from AWCR is directionally propagated to AWCL through the axonal gap junctions that connect contralateral AWB or ASH neurons. These gap junctions could be *nsy-5* independent or *nsy-5* dependent (although NSY-5 puncta were not observed in axons). Genetic mosaic analysis suggests that AWC^{ON} induction in AWCL is stimulated by AWBR-related neurons, which are all on the right side of the animal. Similarly, *odr-3::nsy-5* can rescue AWCL if AWCL and both AWB neurons express *nsy-5.* These results are consistent with a propagation of *nsy-5* information from the right side to the left.

The subthreshold *nsy-4* signal could be propagated from AWCL to AWCR through claudin-like adhesion or other axonal adhesion systems, through midline gap junctions, or through an interaction between NSY-4 and NSY-5 on adjacent cells. The expression pattern of *nsy-4* suggests nonneuronal cells as another possible conduit for cell communication.

The Left-Right Decision

When *nsy-5* activity differs between the two AWC neurons, the cell with more *nsy-5* preferentially becomes AWC^{ON}, and the contralateral cell preferentially becomes AWC^{OFF}. This result indicates that the level of *nsy-5* activity in AWC can bias the left-right decision. In this respect, *nsy-5* is similar to *nsy-4*, a claudin-like protein that has

both autonomous and nonautonomous effects on AWC asymmetry (VanHoven et al., 2006). Unlike *nsy-5* and *nsy-4*, the target genes *unc-43*, *tir-1*, and *nsy-1* affect only the AWC cell that was genetically altered and therefore are implicated in execution of the decision rather than signaling itself (Chuang and Bargmann, 2005; Sagasti et al., 2001).

The two-signal model and the intrinsic bias of *nsy-4* and *nsy-5* suggest that the stochastic event driving random asymmetry may be the relative strengths of the *nsy-5* signal and the *nsy-4* signal when the left and right sides come into contact. The stronger side then generates a feedback signal to the contralateral AWC.

Feedback

Once the two AWC neurons have risen above a signaling threshold, negative feedback is required to suppress the AWC^{ON} state in one cell. We suggest that this feedback is propagated back to the AWC neurons with the cooperation of the other *nsy-5*-expressing cells, perhaps via the *nsy-5* gap junctions.

Overexpression of *nsy-5* in both AWB-related lineages has an unexpected ability to inhibit AWC^{ON} induction in a wild-type background, an effect consistent with a feedback function of AWB-related lineages. A similar feedback function is supported by the targeted rescue of *nsy-5* mutants. Several transgenes rescued AWC^{ON} in *nsy-5* mutants without showing good coordination between the left and right neurons, leading to a large class of 2 AWC^{ON} animals even when there were still many nonrescued 2 AWC^{OFF} animals. This phenotype is expected if signaling can cross the threshold in both AWC neurons but feedback is inefficient. More effective coordination between the two AWCs should be reflected in a dominant 1 AWC^{ON} class at the expense of 2 AWC^{ON} animals, an effect observed when more cells in the AWBR-related lineages were rescued by the *tax-4::nsy-5* transgenes.

Innexin Function in the Developing Nervous System

These results show that immature *C. elegans* neurons are connected in transient gap-junction networks, like many other nascent neural circuits. The *nsy-5* network coordinates sensory specificity, gene expression patterns, and synaptic protein distribution in the left and right AWC neurons by interacting with a calcium channel-CaMKII kinase pathway. In the vertebrate nervous system, synchronous calcium bursts or coupled calcium waves are present at the same time as gap junctions, and some calcium waves require gap junctions to propagate (Kandler and Katz, 1998; Lee et al., 1994; Singer et al., 2001; Yuste et al., 1995). Both gap-junction coupling and hemichannel release of ATP or glutamate can promote calcium wave propagation (Weissman et al., 2004). Since *nsy-5* acts in a well-characterized signaling pathway with conserved molecular targets, the *nsy-5* network could provide insight into other gap-junction networks.

Many of the neurons that express *nsy-5* are synaptically connected in adults (White et al., 1986). Some *nsy-5*-expressing neurons are stably connected by interclass gap junctions (ASH, ADF, ASK, AIZ, ADA, PVQ, and RIC), but most are later linked to each other by chemical synapses. *nsy-5* mutations alter the distribution of AWC synapses in adults, and similarly, innexin mutations can affect chemical synapse formation in *Drosophila* (Curtin et al., 2002). We suggest that the NSY-5 network could extend left-right asymmetry to many neurons by affecting stable patterns of chemical synapses.

EXPERIMENTAL PROCEDURES

Genetics and Molecular Biology

Wild-type strains were *C. elegans* variety Bristol, strain N2. Strains were generated and maintained by standard methods (Brenner, 1974). Complete strain genotypes are listed in Supplemental Experimental Procedures. Standard methods were used for plasmid construction and germline transformation (details in Supplemental Experimental Procedures). For all heterologous expression experiments, DNAs were injected at the same relatively low concentrations (25 ng/μl) and at least three independent transgenic lines were analyzed.

Chemotaxis Assay

Chemotaxis assays were performed as described (Bargmann et al., 1993). Odors were diluted in ethanol and tested at standard concentrations (1:1,000 butanone and 1:10,000 2,3-pentanedione). Three independent assays of each strain were conducted for each odor.

Isolation and Mapping of *nsy-5*

nsy-5(ky634) was isolated from a genetic screen for 2 AWC^{OFF} mutants as described (VanHoven et al., 2006). *nsy-5(ky634)* was mapped on linkage group I between single-nucleotide polymorphisms in the cosmid F23C8 at nucleotide 27234 and Y23H5B at nucleotide 8849 in the CB4856 strain (Washington University School of Medicine, Department of Genetics, Genome Sequencing Center; http://genome.wustl.edu/genome/celegans/chrom1_layout.html). The cDNA clones yk1175f08 and yk383e1, corresponding to *nsy-5a* and *nsy-5b*, respectively, were gifts from Y. Kohara.

NSY-5 Localization in Cultured Mammalian Cells

nsy-5-EGFP was generated by subcloning *nsy-5a* cDNA into the pEGFP-N1 vector (Clontech). COS cells were transfected with *nsy-5*-EGFP using FuGENE transfection reagent (Roche). Fluorescence of NSY-5-EGFP was imaged 36–48 hr after transfection.

Electron Microscopy

N2 and *nsy-5(ky634)* 3-fold embryos and L1 worms were prepared for electron microscopy by high-pressure freezing (HPF) with a Bal-Tec HPM 010 device followed by freeze-substitution (FS) with a Leica AFS. The substitution cocktail contained 1% OsO_4 with 0.2% uranyl acetate in 98% acetone/2% methanol. Samples were substituted for 72 hr at −90°C, warmed to room temperature, and embedded in Eponate 12 resin. Serial sections were examined with a Tecnai T12 microscope and photographed using a Gatan 895 4k × 4k camera and DigitalMicrograph. Membrane orientation was optimized by specimen tilt prior to photography. Measurements were made in DigitalMicrograph, and figures were composed in Adobe Photoshop. Cell IDs were made based on direct tracing of cells and other anatomical features in EM sections and based on 3D models generated from the serial sections using Reconstruct (Fiala, 2005). Three wild-type embryos, two *nsy-5(ky634)* embryos, one wild-type L1, and one *nsy-5(ky634)* L1 were examined.

Expression of *nsy-5* in *Xenopus* Oocytes and Electrophysiological Recordings

nsy-5b was subcloned into the pcDNA3.1 vector (Invitrogen) with a T7 promoter. In vitro transcription, RNA purification, and oocyte injection were performed as described previously (Trexler et al., 2000). To assess the ability of NSY-5 to form hemichannels, single oocytes were recorded in Ringer solution containing 1.8 mM Ca^{2+} ~4 days after RNA injection using a two-electrode voltage clamp (Srinivas et al., 2006; Trexler et al., 2000). To ask whether NSY-5 forms intercellular channels, oocytes were devitellinized 1 day after RNA injection and paired for 1 day before measuring junctional currents with a dual two-electrode voltage clamp (Verselis et al., 1994).

Genetic Mosaic Analysis

The *str-2::GFP*-integrated line *kyIs140 I* in wild-type or *nsy-5(ky634)* animals was injected with DNA for *nsy-5(genomic)*, *odr-1::DsRed*, and *ofm-1::GFP* or *odr-3::nsy-5*, *odr-1::dsRed*, and *ofm-1::GFP*. Mosaic analysis and statistical analysis were performed as previously described (Sagasti et al., 2001; VanHoven et al., 2006). Transgenic lines were passed for six generations to allow the transgenes to stabilize before screening for mosaics. The presence of the extrachromosomal array was visible in the AWC and AWB neurons, which expressed the coinjection marker *odr-1::DsRed*. Expected numbers of mosaic animals were generated from internal control animals, which retained the *nsy-5* transgene in both AWC neurons, from the same transgenic line. Expected and observed numbers of mosaic animals in each class were compared using the chi-square test with three degrees of freedom. Statistical analysis supports a lateral interaction model in which the cell with higher *nsy-5* activity becomes AWC^{ON} and the cell with lower *nsy-5* activity becomes AWC^{OFF}: p = 0.10–0.25 (rescue line 1), 0.25–0.5 (rescue line 2), 0.1–0.25 (rescue line 3), 0.02–0.05 (gain-of-function line 1), and 0.10–0.25 (gain-of-function line 4). Statistical analysis was also used to test an execution model in which *nsy-5* acts strictly cell autonomously in a permissive fashion (i.e., a wild-type cell becomes AWC^{ON} and AWC^{OFF} with equal frequency, a *nsy-5(lf)* cell becomes AWC^{OFF}, and a *nsy-5(OE)* cell becomes AWC^{ON}). In all cases, $p < 0.001$, excluding the model.

Supplemental Data

Supplemental Data include Supplemental Experimental Procedures, Supplemental References, two tables, and three figures and can be found with this article online at http://www.cell.com/cgi/content/full/129/4/787/DC1/.

ACKNOWLEDGMENTS

We are grateful to K. McDonald of the University of California, Berkeley and K.D. Derr at the New York Structural Biology Center for assistance in the freezing of embryos. We thank C. Woods and H. Jaramillo for excellent technical support and S. Bauer Huang, C. Chang, B. Lesch, M. Tsunozaki, M. Zimmer, N. Pokala, G. Lee, and A. Chang for comments, discussions, and reagents. We also thank A. North and the Rockefeller University Bio-Imaging Resource Center for advice on confocal imaging, S. McCarroll for the pSM and pSM-GFP vectors, S. Kennedy and G. Ruvkun for the *eri-1;lin-15B* strain, Y. Kohara for EST clones, A. Fire for *C. elegans* vectors, T. Stiernagle and the Caenorhabditis Genetic Center for strains, S. Mitani for *nsy-5(tm1896)*, and WormBase. This work was supported by NIH grant RO1 DC04089. C.I.B. is an Investigator of the Howard Hughes Medical Institute.

Received: September 28, 2006
Revised: January 27, 2007
Accepted: February 26, 2007
Published: May 17, 2007

REFERENCES

Bargmann, C.I., Hartwieg, E., and Horvitz, H.R. (1993). Odorant-selective genes and neurons mediate olfaction in *C. elegans*. Cell *74*, 515–527.

Bauer, R., Lehmann, C., Martini, J., Eckardt, F., and Hoch, M. (2004). Gap junction channel protein innexin 2 is essential for epithelial morphogenesis in the *Drosophila* embryo. Mol. Biol. Cell *15*, 2992–3004.

Bennett, M.V., and Zukin, R.S. (2004). Electrical coupling and neuronal synchronization in the mammalian brain. Neuron *41*, 495–511.

Brenner, S. (1974). The genetics of *Caenorhabditis elegans*. Genetics *77*, 71–94.

Bruzzone, R., Hormuzdi, S.G., Barbe, M.T., Herb, A., and Monyer, H. (2003). Pannexins, a family of gap junction proteins expressed in brain. Proc. Natl. Acad. Sci. USA *100*, 13644–13649.

Chang, Q., Gonzalez, M., Pinter, M.J., and Balice-Gordon, R.J. (1999). Gap junctional coupling and patterns of connexin expression among neonatal rat lumbar spinal motor neurons. J. Neurosci. *19*, 10813–10828.

Chuang, C.F., and Bargmann, C.I. (2005). A Toll-interleukin 1 repeat protein at the synapse specifies asymmetric odorant receptor expression via ASK1 MAPKKK signaling. Genes Dev. *19*, 270–281.

Curtin, K.D., Zhang, Z., and Wyman, R.J. (2002). Gap junction proteins expressed during development are required for adult neural function in the *Drosophila* optic lamina. J. Neurosci. *22*, 7088–7096.

Ebihara, L., and Steiner, E. (1993). Properties of a nonjunctional current expressed from a rat connexin46 cDNA in Xenopus oocytes. J. Gen. Physiol. *102*, 59–74.

Fiala, J.C. (2005). Reconstruct: a free editor for serial section microscopy. J. Microsc. *218*, 52–61.

Hobert, O., Johnston, R.J., Jr., and Chang, S. (2002). Left-right asymmetry in the nervous system: the *Caenorhabditis elegans* model. Nat. Rev. Neurosci. *3*, 629–640.

Kamath, R.S., Martinez-Campos, M., Zipperlen, P., Fraser, A.G., and Ahringer, J. (2001). Effectiveness of specific RNA-mediated interference through ingested double-stranded RNA in *Caenorhabditis elegans*. Genome Biol. *2*, RESEARCH0002.

Kandler, K., and Katz, L.C. (1995). Neuronal coupling and uncoupling in the developing nervous system. Curr. Opin. Neurobiol. *5*, 98–105.

Kandler, K., and Katz, L.C. (1998). Coordination of neuronal activity in developing visual cortex by gap junction-mediated biochemical communication. J. Neurosci. *18*, 1419–1427.

Landesman, Y., White, T.W., Starich, T.A., Shaw, J.E., Goodenough, D.A., and Paul, D.L. (1999). Innexin-3 forms connexin-like intercellular channels. J. Cell Sci. *112*, 2391–2396.

Lee, S.H., Kim, W.T., Cornell-Bell, A.H., and Sontheimer, H. (1994). Astrocytes exhibit regional specificity in gap-junction coupling. Glia *11*, 315–325.

Levin, M., and Mercola, M. (1999). Gap junction-mediated transfer of left-right patterning signals in the early chick blastoderm is upstream of Shh asymmetry in the node. Development *126*, 4703–4714.

Li, S., Dent, J.A., and Roy, R. (2003). Regulation of intermuscular electrical coupling by the *Caenorhabditis elegans* innexin *inx-6*. Mol. Biol. Cell *14*, 2630–2644.

Liu, Q., Chen, B., Gaier, E., Joshi, J., and Wang, Z.W. (2006). Low conductance gap junctions mediate specific electrical coupling in body-wall muscle cells of *Caenorhabditis elegans*. J. Biol. Chem. *281*, 7881–7889.

Phelan, P. (2005). Innexins: members of an evolutionarily conserved family of gap-junction proteins. Biochim. Biophys. Acta *1711*, 225–245.

Phelan, P., Stebbings, L.A., Baines, R.A., Bacon, J.P., Davies, J.A., and Ford, C. (1998). *Drosophila* Shaking-B protein forms gap junctions in paired *Xenopus* oocytes. Nature *391*, 181–184.

Rongo, C., and Kaplan, J.M. (1999). CaMKII regulates the density of central glutamatergic synapses in vivo. Nature *402*, 195–199.

Saez, J.C., Retamal, M.A., Basilio, D., Bukauskas, F.F., and Bennett, M.V. (2005). Connexin-based gap junction hemichannels: gating mechanisms. Biochim. Biophys. Acta *1711*, 215–224.

Sagasti, A., Hisamoto, N., Hyodo, J., Tanaka-Hino, M., Matsumoto, K., and Bargmann, C.I. (2001). The CaMKII UNC-43 activates the MAPKKK NSY-1 to execute a lateral signaling decision required for asymmetric olfactory neuron fates. Cell *105*, 221–232.

Sieburth, D., Ch'ng, Q., Dybbs, M., Tavazoie, M., Kennedy, S., Wang, D., Dupuy, D., Rual, J.F., Hill, D.E., Vidal, M., et al. (2005). Systematic analysis of genes required for synapse structure and function. Nature *436*, 510–517.

Singer, J.H., Mirotznik, R.R., and Feller, M.B. (2001). Potentiation of L-type calcium channels reveals nonsynaptic mechanisms that correlate spontaneous activity in the developing mammalian retina. J. Neurosci. *21*, 8514–8522.

Srinivas, M., Calderon, D.P., Kronengold, J., and Verselis, V.K. (2006). Regulation of connexin hemichannels by monovalent cations. J. Gen. Physiol. *127*, 67–75.

Starich, T., Sheehan, M., Jadrich, J., and Shaw, J. (2001). Innexins in *C. elegans*. Cell Commun. Adhes. *8*, 311–314.

Starich, T.A., Lee, R.Y., Panzarella, C., Avery, L., and Shaw, J.E. (1996). *eat-5* and *unc-7* represent a multigene family in *Caenorhabditis elegans* involved in cell-cell coupling. J. Cell Biol. *134*, 537–548.

Starich, T.A., Miller, A., Nguyen, R.L., Hall, D.H., and Shaw, J.E. (2003). The *Caenorhabditis elegans* innexin INX-3 is localized to gap junctions and is essential for embryonic development. Dev. Biol. *256*, 403–417.

Stebbings, L.A., Todman, M.G., Phelan, P., Bacon, J.P., and Davies, J.A. (2000). Two *Drosophila* innexins are expressed in overlapping domains and cooperate to form gap-junction channels. Mol. Biol. Cell *11*, 2459–2470.

Stebbings, L.A., Todman, M.G., Phillips, R., Greer, C.E., Tam, J., Phelan, P., Jacobs, K., Bacon, J.P., and Davies, J.A. (2002). Gap junctions in *Drosophila*: developmental expression of the entire innexin gene family. Mech. Dev. *113*, 197–205.

Tanaka-Hino, M., Sagasti, A., Hisamoto, N., Kawasaki, M., Nakano, S., Ninomiya-Tsuji, J., Bargmann, C.I., and Matsumoto, K. (2002). SEK-1 MAPKK mediates Ca2+ signaling to determine neuronal asymmetric development in *Caenorhabditis elegans*. EMBO Rep. *3*, 56–62.

Trexler, E.B., Bukauskas, F.F., Kronengold, J., Bargiello, T.A., and Verselis, V.K. (2000). The first extracellular loop domain is a major determinant of charge selectivity in connexin46 channels. Biophys. J. *79*, 3036–3051.

Troemel, E.R., Sagasti, A., and Bargmann, C.I. (1999). Lateral signaling mediated by axon contact and calcium entry regulates asymmetric odorant receptor expression in *C. elegans*. Cell *99*, 387–398.

VanHoven, M.K., Bauer Huang, S.L., Albin, S.D., and Bargmann, C.I. (2006). The claudin superfamily protein *nsy-4* biases lateral signaling to generate left-right asymmetry in *C. elegans* olfactory neurons. Neuron *51*, 291–302.

Verselis, V.K., Ginter, C.S., and Bargiello, T.A. (1994). Opposite voltage gating polarities of two closely related connexins. Nature *368*, 348–351.

Wei, C.J., Xu, X., and Lo, C.W. (2004). Connexins and cell signaling in development and disease. Annu. Rev. Cell Dev. Biol. *20*, 811–838.

Weissman, T.A., Riquelme, P.A., Ivic, L., Flint, A.C., and Kriegstein, A.R. (2004). Calcium waves propagate through radial glial cells and modulate proliferation in the developing neocortex. Neuron *43*, 647–661.

Wes, P.D., and Bargmann, C.I. (2001). *C. elegans* odour discrimination requires asymmetric diversity in olfactory neurons. Nature *410*, 698–701.

White, J.G., Southgate, E., Thomson, J.N., and Brenner, S. (1986). The structure of the nervous system of *Caenorhabditis elegans*. Philos. Trans. R. Soc. Lond. B Biol. Sci. *314*, 1–340.

Yuste, R., Nelson, D.A., Rubin, W.W., and Katz, L.C. (1995). Neuronal domains in developing neocortex: mechanisms of coactivation. Neuron *14*, 7–17.

Zampighi, G., Corless, J.M., and Robertson, J.D. (1980). On gap junction structure. J. Cell Biol. *86*, 190–198.

Site Map
Documentation
Guidelines

ACTION : Preview ! : ACTION

pubID : 00029404
curator : Tuco
reference : author == Chuang CF author == Vanhoven MK author == Fetter RD author == Verselis VK author == Bargmann CI identifier == pmid17512411 title == An Innexin-Dependent Cell Network Establishes Left-Right Neuronal Asymmetry in C. elegans. journal == Cell volume == 129 pages == 787//799 year == 2007 abstract == Gap junctions are widespread in immature neuronal circuits, but their functional significance is poorly understood. We show here that a transient network formed by the innexin gap-junction protein NSY-5 coordinates left-right asymmetry in the developing nervous system of Caenorhabditis elegans. nsy-5 is required for the left and right AWC olfactory neurons to establish stochastic, asymmetric patterns of gene expression during embryogenesis. nsy-5-dependent gap junctions in the embryo transiently connect the AWC cell bodies with those of numerous other neurons. Both AWCs and several other classes of nsy-5-expressing neurons participate in signaling that coordinates left-right AWC asymmetry. The right AWC can respond to nsy-5 directly, but the left AWC requires nsy-5 function in multiple cells of the network. NSY-5 forms hemichannels and intercellular gap-junction channels in Xenopus oocytes, consistent with a combination of cell-intrinsic and network functions. These results provide insight into gap-junction activity in developing circuits.
genesymbol : nsy-5=inx-19
genefunction : nsy-5=inx-19 forms gap-junction channels in xenopus oocytes fig.5
expression : fig.4
rnai : yes
transgene : in methods
overexpression : nsy-5=inx-19 overexpression fig.2
mosaic : nsy-5=inx-19 mosaic fig.6G
site : nsy-5=inx-19 site of action fig.6
newmutant : nsy-5=inx-19
sequencechange : nsy-5=inx-19 mutation in fig.1
geneinteractions : nsy-5=inx-19, unc-2
supplemental : yes

Update !

ACTION : Preview ! : ACTION

Curation Fields 4,232 Papers